PHYSICAL REVIEW B
CONDENSED MATTER

THIRD SERIES, VOLUME 47, NUMBER 5 1 FEBRUARY 1993-I

Phosphorus-induced relaxation in an iron grain boundary: A cluster-model study

Shaoping Tang and A. J. Freeman
Department of Physics and Astronomy, Northwestern University, Evanston, Illinois 60208

G. B. Olson
Department of Materials Science and Engineering, Northwestern University, Evanston, Illinois 60208
(Received 14 August 1992)

The DMol molecular-cluster method, based on local density-functional theory, is employed to study the electronic structure and structural relaxation of a P impurity in the Fe $\Sigma 3[1\bar{1}0](111)$ grain boundary (GB). Large clusters (53 and 91 atoms) are used to simulate the local environment of the Fe grain boundary; by calculating the force on the nearby Fe atoms around the impurity and minimizing the total energy of the cluster, an optimized atomic geometry with minimum energy is obtained. In the pure grain boundary, the center Fe atoms above the GB core have the tendency to move toward each other keeping a bond length very close to the Fe bulk bond length. From the 91-atom cluster, the P-induced relaxation of the Fe GB extends to at least eight Fe layers and the bond length between P and the nearest vertical Fe is 2.34 Å, which is 3.5% larger than that in bulk Fe_3P. Although the nearest Fe-P distance is the same in the vertical and horizontal directions, we found a stronger bonding between P and the in-plane Fe than in the vertical direction, which may contribute to the P embrittlement of Fe. A lesson from the present study with two cluster models is that even a cluster as large as 53 atoms does not provide the correct bonding picture around the impurity. This is due to the large relaxation induced by the P atom, which cannot be treated by a 53-atom cluster.

I. INTRODUCTION

Understanding the different role of boron, carbon, and phosphorus in the embrittlement of iron is very important for the design of stress-corrosion resistant high-strength steels.[1] It is known that carbon and boron enhance the intergranular cohesion in iron and steels, while phosphorus tends to embrittle. The precise mechanism underlying this phenomenon is not well known, although there exists quite a number of experimental and theoretical studies.[2–14] The theoretical efforts made so far are very useful in helping to elucidate this problem. Because of its computational complexity, however, there is one basic problem that every theoretical method has to face, i.e., how to choose a geometry that correctly describes the real Fe grain boundary (GB) with and without impurities. Most theoretical calculations have simply assumed a geometry in order to perform calculations.[6,7]

Previous electronic structure studies[8–11] used small cluster models (< 10 atoms) to simulate the local environment of impurities such as B, C, P, and S in a metal grain boundary (Fe, Ni, etc.) and provided useful information with which to understand the bonding between the metal and impurities. Thus, Messmer[8] found that there are considerable bonding interactions between the metalloid (B or P) atoms and the metal atoms of the cluster. Later cluster calculations by Painter and Averill[10] revealed that B increases the maximum sustainable restoring force in the Ni cluster and S decreases this force, in agreement with the observed segregation behavior of these atoms. Collins, O'Handley, and Johnson[11] studied the Fe_4-M (M=B, C, Si, N) cluster with self-consistent-field $X\alpha$ scattered-wave molecular-orbital calculations and found that there are two types of bonding between Fe and M, i.e., polar s-d and covalent p-d bonding and that polar bonding plays a greater role in the overall stability than does covalent bonding. Eberhart and Vvedensky[12] also discussed the role of certain segregated impurities as inhibitors of intergranular brittleness of some $L1_2$ intermetallic compounds.

Because those studies employed small cluster models, the structural changes when impurities are introduced cannot be determined. In this paper, we report studies of the structural and electronic changes when P is intro-

duced in the Fe $\Sigma 3[1\bar{1}0](111)$ grain boundary. We will show that the relaxation of the atomic geometry of the GB due to the impurity atom may cause a several eV decrease in the total binding energy. The atomic relaxation is found to extend over at least eight layers of Fe (assuming the center layer is in the zero layer) above the impurity atom so that an assumed unrelaxed structure may not give an accurate description of the electronic structure of impurities in the iron GB. The major difficulty in obtaining a correct geometry from conventional energy-band approaches comes from the fact that since there is a large relaxation of the Fe grain boundary with and without the impurities, a very large unit cell must be set up in order to simulate such relaxation. Furthermore, to obtain an optimized structure, a trial and error method is used (if an atomic force calculation is not available) that requires at least an order of magnitude increase in computer time. In practice, this is prohibitively expensive. One way to partially overcome this difficulty is to use some relatively less accurate approach such as an empirical method to overcome the computer time requirements. Examples of this are calculations using the embedded atom method (EAM) by Harrison *et al.*[13] and Krasko.[14] Another way would be to maintain the first principles method but to calculate the force on each atom to guide the movement of atoms. Thus, we chose the DMol approach[15] which is a first principles method based on density functional theory that is capable of giving the force acting on each atom. Another virtue of this method is that it enables the use of large cluster models to simulate the real system. As is well known, the molecular-cluster model represents a convenient way of studying those electronic properties that are primarily a function of the local environment of the system, such as vacancies, impurities, and local moments.

II. METHODOLOGY

We use the DMol method[15] which, as stated, is a first-principles numerical method for solving the local density functional equations and is capable of calculating analytic energy gradients[16] for each atom within the cluster model. While details of the DMol method have been published elsewhere, some technical details regarding the calculation are provided below. The Hedin-Lundqvist exchange correlation potential[17] is employed with the frozen-core approximation. We use extended basis sets for the P and Fe atoms, i.e., a double set of valence functions plus a single d polarization function for P and a single p function for Fe. The binding energy of a cluster is defined as $E_b = E_t - E_a$, where E_t is the total energy of the cluster and the E_a is the sum of atomic energies. For a given atomic geometry, the binding energy of the system and the forces on atoms of interest are calculated. To find the optimized geometry, the atoms are further displaced according to the forces acting on them. An optimized structure is obtained when all the forces acting on the atom are sufficiently small. In this work, the degree of convergence is measured by root-mean-square (rms) changes in the charge density. It is set to 10^{-5} which allows the total energy to converge to 10^{-5} Ry. The force convergence criterion is 6.0×10^{-3} (Ry/a.u.).

Two cluster models having 53 and 91 atoms (shown in Fig. 1) are used to simulate P in the Fe GB with the P atom placed at the center of the trigonal prism formed by iron atoms in the GB core. The 91-atom cluster contains 17 layers of Fe (from the point of view of a slab model) and is probably the largest cluster ever chosen to represent a metal grain boundary problem. By examining the GB structure, it is obvious that only those atoms in columns 1 and 2 are most affected by impurities in the center of the GB (see Fig. 1). In determining the optimum geometry, the boundary atoms of the cluster are fixed in their bulk position. For the 53-atom cluster, only atoms in the same layer with Fe_{11} and Fe_{21} are allowed to move. For the 91-atom cluster, the atoms in the same layer of Fe_{12} and Fe_{22} are also allowed to move. The D_{3h} symmetry is used for the two cluster models. In this pa-

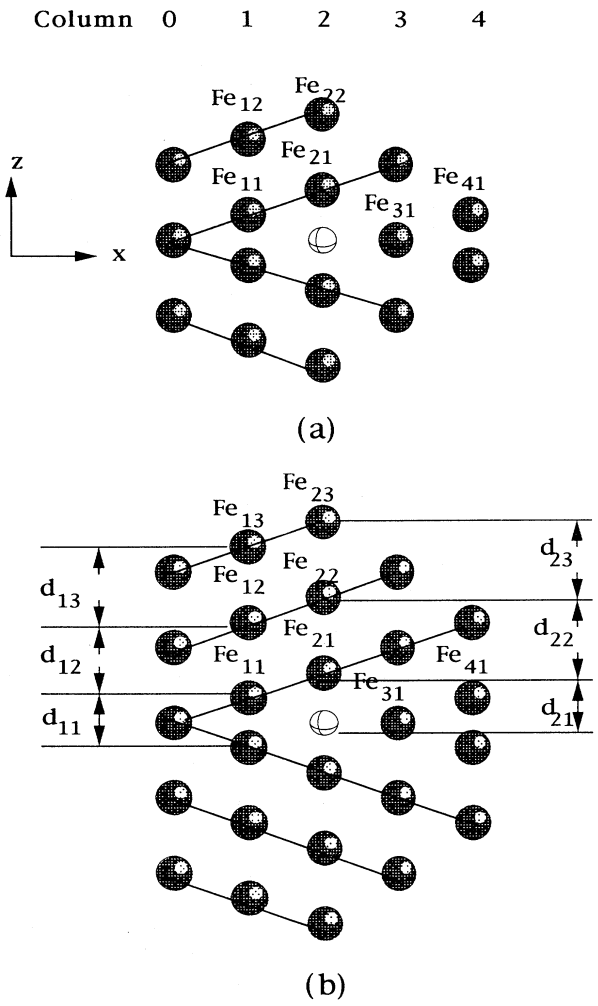

FIG. 1. Side view of the Fe $\Sigma 3[1\bar{1}0](111)$ grain boundary represented in the two cluster models studied. The P atom (open circle) is put in the center of the trigonal prism formed by Fe atoms in the GB core. Atoms in each Fe layer are not shown in the figure. (a) Cluster of 53 atoms and (b) cluster of 91 atoms.

per, when we refer to relaxation of a particular atom, other atoms satisfying D_{3h} group operations have the same amount of relaxation.

III. RESULTS AND DISCUSSION

A. 53-atom cluster model

Initially, the relaxation of the pure GB without P is determined. Note that while the corresponding atoms in columns 1 and 4 of Fig. 1 are identical in an infinite GB, in the present cluster-model atoms in column 4 are boundary atoms. If they are placed according to their bulk positions, it is apparent that the distances between the two near-center atoms in columns 1 and 4 (Fe_{11} and Fe_{41}) are too small (33% smaller than the ideal bulk value) and the distances between two near-center atoms in column 2 (Fe_{21}) are too large (33% larger than the ideal bulk value). Atomic relaxation is needed to make the structure stable. Since it is expected that the local environment of P is less affected by atoms in column 4, the bond length between two near-center Fe atoms in column 4 is fixed at 2.22 Å which corresponds to zero force along the z direction in the 53-atom cluster; when we also change this distance to 2.06 and 1.85 Å, it turns out that the forces acting on Fe_{11} and Fe_{21} atoms remain almost the same.

The calculated optimized structure information for the ideal GB, the relaxed GB, and P in the relaxed GB are displayed in Table I. For the ideal GB structure, the calculated force on Fe_{11} is a large repulsive force and the force on Fe_{21} is an attractive force indicating that the Fe_{21} atom tends to move towards the center of the GB. The final optimized structure is obtained when the Fe_{21} atom is a little below the Fe_{11} plane (referred to as GB-1). Another structure with an energy minimum is found by moving Fe_{21} away from the center and forming a short interlayer distance with the fifth layer ($d_{22}=2.12$ Å) (referred to as GB-2). Since the binding energy of GB-1 is about 1.1 eV lower than that of GB-2, the GB-1 structure is clearly more stable than the metastable GB-2 structure.

When P is added at the center of the ideal GB, there is a strong tendency that Fe layers above P are pushed away from the center plane. By moving Fe_{11} and Fe_{21} according to the force along the z direction and minimizing this force, it is found that the forces between the in-plane atoms are also minimized. This shows that the relaxation of the Fe GB is mainly along the z direction. The binding energy of the optimized structure of P in the GB (GB-P) is 5.9 eV greater than that of GB-1, which corresponds to an energy lowering of 0.74 eV per relaxed atom. This optimized structure shows that the distance between two Fe_{11} atoms (d_{11}) is stretched and approaches the bulk Fe—Fe bond length (2.48 Å) and that the Fe_{21} atom directly above P relaxes 30% outward compared with its ideal position resulting in an Fe—P bond length of 2.16 Å.

In this configuration, the charge density difference plotted in a plane containing P and several neighboring Fe atoms is shown in Fig. 2. (The charge density difference is calculated by subtracting from the density of GB-P the pure GB density and a single P density placed at the center of the GB so that the P-induced charge redistribution is clearly shown.) It is seen that P serves as a charge donor which contradicts electronegativity considerations. Such a "reverse" charge transfer was found in previous linearized muffin-tin orbital method (LMTO-ASA) (Ref. 6) and full potential linearized augmented plane wave (Ref. 7) calculations of P in the Fe GB and also in other systems such as PdB (Ref. 18) and Ni_3P.[19] The bonding between P and Fe in the vertical direction is a little stronger than that in the horizontal direction. This is due to the smaller Fe—P bond length in the vertical direction. The LMTO-ASA calculation[6] used a unit cell of eight atoms, set the Fe—P bond length to be 2.26 Å and showed a comparable interaction between P and Fe in both directions. We found that the same con-

TABLE I. The structural parameters (in Å) shown in Fig. 1 calculated from a 53-atom cluster model. The "ideal" distances are calculated from the unrelaxed GB structure. GB-1 refers to the geometry when Fe_{21} relaxes inward towards the center of the GB and GB-2 refers to the geometry when Fe_{21} relaxes outward, GB-P refers to the case when P is added to the GB, d_{Fe} is the distance between the two near-center atoms in column 2 in the pure GB and E_b is the binding energy in eV.

	Ideal	GB-1	GB-2	GB-P
d_{11}	1.65	2.50	2.35	2.41
d_{12}	2.48	2.06	2.14	2.10
d_{21}	. . .	. . .	. . .	2.16
d_{22}	2.48	2.91	2.12	1.97
d_{Fe}	3.31	2.46	4.04	. . .
E_b	−220.20	−225.75	−224.67	−231.65

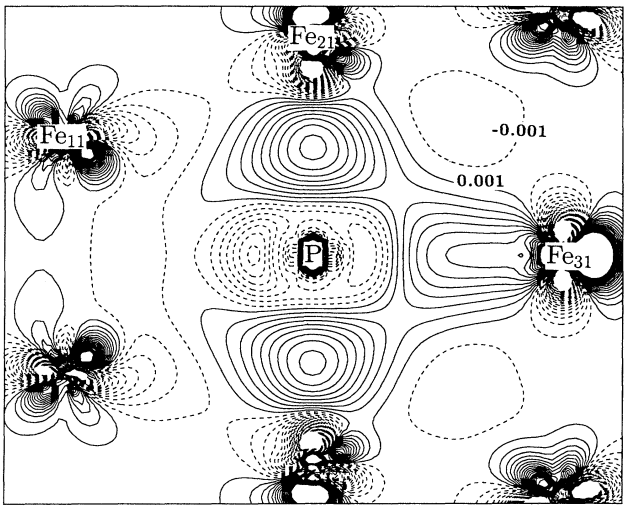

FIG. 2. Charge density difference between P in the GB and a superposition of a single P and pure GB calculated from the 53-atom cluster. The vertical Fe—P bond length is 2.16 Å. The plots are in a plane containing P, Fe_{11}, Fe_{21}, and Fe_{31}. The contour spacings are $0.002e/(\text{a.u.})^3$. Solid lines mean charge gain, dashed lines mean charge loss.

clusion can be reached when we change the P—Fe_{21} bond length to 2.23 Å. Since the competition between bonding in the vertical and horizontal directions is an important factor in studying the mechanism of embrittlement, the present bonding picture calculated from the 53 atom cluster may not appear to support the P embrittlement of Fe.

This discrepancy can be understood by examining the optimized structure shown in Table I. It is obvious that the distances between inner Fe atoms and the boundary Fe atoms in the 53-atom cluster (e.g., d_{12} and d_{22}) are very much compressed compared to the ideal value, which does not reflect reality because the boundary atoms are purposely fixed in their bulk positions. Actually, Fe_{12} and Fe_{22} may move outward since there is a large relaxation of the inner Fe atoms and this movement may also affect the inner Fe atoms. Indeed, when Fe_{12} and Fe_{22} relax outward by 0.1 Å, the inner Fe_{11} and Fe_{21} atoms also move in the same direction, but the question how far they can go cannot be answered by the present small cluster model.

B. 91-atom cluster model

A more realistic simulation of the local environment around P is very desirable, since the nearest distance between Fe and P is the key factor for evaluating the interaction between Fe and P. Therefore, a cluster of 91 atoms—which expands three Fe layers along both the $+z$ and $-z$ directions from the 53-atom cluster—is chosen. The same computational procedure described above for the smaller cluster is employed. The structural parameters of the optimized structure are shown in Table II. For the pure GB, as in the case of 53 atoms, two energy minima are found: one is above the third layer plane (GB-1) and the other is below the first layer leading to an Fe-Fe distance of 2.43 Å which is smaller than that in the 53-atom case. Again, GB-1 is more stable energetically than GB-2.

When P is introduced in the GB center, the Fe-P distance expands to 2.34 Å, which is a large increase compared to the 2.16 Å value for the 53-atom cluster. This shows that the relaxation of Fe_{22} really affects the interaction between P and the nearest Fe atoms. The energy lowering on adding P to Fe GB is 6.24 eV ($\sim$0.39 eV per relaxed atom) which is larger than the 5.9 eV in the small cluster case. This is expected because more atoms take part in the relaxation procedure.

TABLE II. The structural parameters (in Å) shown in Fig. 1 calculated from a 91-atom cluster model. GB-1, GB-2, GB-P, d_{Fe}, and E_b (in eV) have the same meaning as in Table I.

	Ideal	GB-1	GB-2	GB-P
d_{11}	1.65	2.49	2.52	2.57
d_{12}	2.48	2.47	2.39	2.37
d_{13}	2.48	2.07	2.14	2.14
d_{21}	...	...	...	2.34
d_{22}	2.48	2.48	2.30	2.31
d_{23}	2.48	2.93	1.99	1.97
d_{Fe}	3.31	2.43	4.66	...
E_b	...	−421.86	−419.98	−428.10

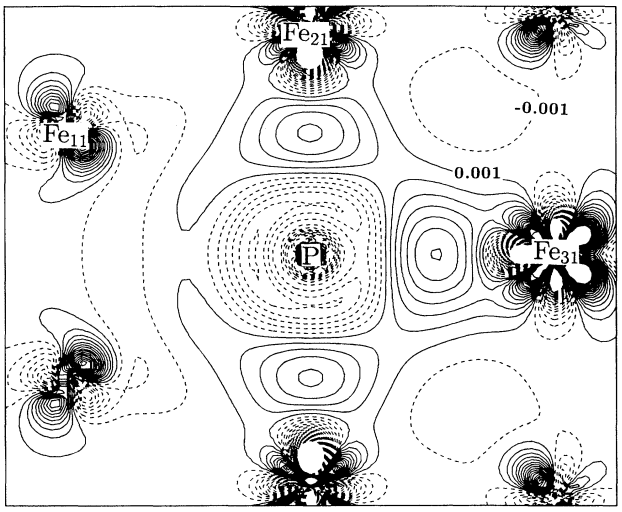

FIG. 3. Charge density difference calculate from the 91-atom cluster. The vertical Fe—P bond length is 2.34 Å. The plot is in the same plane as in Fig. 2.

Let us now examine in Fig. 3 the charge density difference obtained for the large cluster. The common feature of this figure with Fig. 2 is that P transfers some charge to the nearby Fe atoms leading to a polarized bonding between Fe and P. While the Fe—P bonding in the horizontal direction does not change too much, the interaction between P and the vertical Fe is greatly decreased because of the increased distance between P and Fe_{21}. This is clear evidence that the P impurity has stronger in-plane interaction with Fe.

It is essential to note that the distances between boundary and inner Fe atoms (d_{13} and d_{23}) are still very much compressed compared with the ideal bulk near-neighbor length implying that the boundary atoms will move outward if an even larger cluster is used. However, the relative bonding strength of P and Fe along the vertical and horizontal directions will not change. An important difference between P-induced relaxation of the Fe GB and the relaxation of metal or semiconductor free surfaces is that the former relaxation decays slowly along the direction perpendicular to the center GB plane while the latter usually damps rapidly within several atomic layers. This situation makes the theoretical study of P at the Fe GB much more difficult because one needs to construct a large supercell in the band structure method or to use a rather large cluster to include the relaxation effects of the outer Fe layers. An alternative way to deal with such a system is to use a smaller unit cell or cluster but to take the optimized structural information shown in Table II for the corresponding atoms. In this way, one neglects the relaxation of the outer Fe layer, but the local environment around the impurity is properly handled. For example, we have used the coordinate information given in Table II in a new calculation with 53 atoms and the results reproduce correctly the strong horizontal P—Fe bonding compared to vertical bonding. This gives us confidence in further studying other properties of P at the

Fe GB using a smaller cluster or unit cell.

Finally, it is worthwhile to compare the present relaxation study with an empirical calculation using a modified embedded atom method by Krasko.[14] The major difference is that we found two clean GB structures having energy minima corresponding to the up and down displacements of the third layer atom (Fe_{21}), whereas the EAM calculation gave one clean GB structure representing the down position of Fe_{21}. There are some similar points between the two calculations. For example, they both found that the atomic relaxation is large in several layers of Fe relative to the center plane for either clean or P-doped GBs. By adding P into the GB center, both studies showed that the first (Fe_{11} plane) and second (Fe_{21} plane) layer of Fe atoms are relaxed away from the center plane. The nearest Fe-P distance across the GB is 2.34 Å from the present study which is in agreement with 2.5 Å from the EAM result.[20] The virtue of the EAM study[14] is that it can include a large number of atoms into the calculation without demanding too much computing power, which is beyond the present capability of first-principles calculation. As is shown in Ref. [14], Krasko found that relaxation still exists for the 10th layer by including up to 13 Fe layers above the center GB plane in the calculation. In view of the similarity between the two results when the impurity resides in the Fe GB, the first-principles calculations can use the EAM data[14] as the first step calculation.

ACKNOWLEDGMENTS

We are pleased to acknowledge helpful discussions with Dr. R. Wu. This work was supported by the Office of Naval Research (Grant No. N00014-90-J-1363) and by the NSF Division for Advanced Scientific Computing at the Pittsburgh Supercomputing Center.

[1]G. B. Olson, in *Innovations in Ultrahigh-Strength Steel Technology,* edited by G. B. Olson, M. Azrin, and E. S. Wright, Sagamore Army Material Research Conference Proceedings: 34th (1987), p. 3, and references therein.

[2]C. J. McMahon, Jr., in *Innovations in Ultrahigh-Strength Steel Technology,* edited by G. B. Olson, M. Azrin, and E. S. Wright, Sagamore Army Material Research Conference Proceedings: 34th (1987), p. 597.

[3]P. M. Anderson, J-S. Wang, and J. R. Rice, in *Innovations in Ultrahigh-Strength Steel Technology,* edited by G. B. Olson, M. Azrin, and E. S. Wright, Sagamore Army Material Research Conference Proceedings: 34th (1987), p. 619.

[4]M. E. Eberhart and J. M. MacLaren, in *Innovations in Ultrahigh-Strength Steel Technology,* edited by G. B. Olson, M. Azrin, and E. S. Wright, Sagamore Army Material Research Conference Proceedings: 34th (1987), p. 693.

[5]J. R. Rice and J-S. Wang, Mat. Sci. Eng. A **107**, 23 (1989).

[6]G. L. Krasko and G. B. Olson, Solid State Commun. **76**, 247 (1990).

[7]R. Wu, A. J. Freeman, and G. B. Olson, J. Mater. Res. **7**, 2403 (1992).

[8]R. P. Messmer, Phys. Rev. B **23**, 1616 (1981).

[9]R. P. Messmer and C. L. Briant, Acta Metall. **30**, 457 (1982).

[10]G. S. Painter and F. W. Averill, Phys. Rev. Lett. **58**, 234 (1987).

[11]A. Collins, R. C. O'Handley, and K. H. Johnson, Phys. Rev. B **38**, 3665 (1988).

[12]M. E. Eberhart and D. D. Vvedensky, Phys. Rev. Lett. **58**, 61 (1987).

[13]R. J. Harrison, F. Spaepen, A. F. Voter, and S-P. Chen, in *Innovations in Ultrahigh-Strength Steel Technology,* edited by G. B. Olson, M. Azrin, and E. S. Wright, Sagamore Army Material Research Conference Proceedings: 34th (1987), p. 651.

[14]G. L. Krasko, in *Structure and Properties of Interface in Materials,* edited by W. A. T. Clark, U. Dahmen, and C. L. Briant, MRS Symposia Proceedings No. 238 (Materials Research Society, Pittsburgh, 1991), p. 481.

[15]B. Delley, J. Chem. Phys. **92**, 508 (1990).

[16]B. Delley, J. Chem. Phys. **94**, 7245 (1991).

[17]L. Hedin and B. I. Lundqvist, J. Phys. C **4**, 2064 (1971).

[18]C. D. Gelatt, Jr., A. R. Williams, and V. L. Moruzzi, Phys. Rev. B **27**, 2005 (1983).

[19]S. S. Jaswal, Phys. Rev. B **34**, 8937 (1987).

[20]Here the value of Fe—P bond length is read from Fig. 3 of Ref. 14.